Nuclear Instruments and Methods in Physics Research A ∎ (∎∎∎∎) ∎∎∎–∎∎∎

Contents lists available at ScienceDirect

Nuclear Instruments and Methods in Physics Research A

journal homepage: www.elsevier.com/locate/nima

Formation and stability of a hollow electron beam in the presence of a plasma wake field driven by an ultra-short electron bunch

F. Tanjia [a,b,*], R. Fedele [a,b], S. De Nicola [a,b,c], T. Akhter [a,b], D. Jovanović [d]

[a] Dipartimento di Fisica, Università di Napoli "Federico II", Italy
[b] INFN Sezione di Napoli, Italy
[c] CNR-SPIN, Complesso Universitario di Monte S'Angelo, Napoli, Italy
[d] Institute of Physics, University of Belgrade, Belgrade, Serbia

ARTICLE INFO

Article history:
Received 13 November 2015
Received in revised form
1 April 2016
Accepted 1 April 2016

Keywords:
Plasma wake field generation
Ultrashort electron bunches
Hollow electron beam
Thermal wave model
Quantum-like description

ABSTRACT

A numerical investigation on the spatiotemporal evolution of an electron beam, externally injected in a plasma in the presence of a plasma wake field, is carried out. The latter is driven by an ultra-short relativistic axially-symmetric femtosecond electron bunch. We first derive a novel Poisson-like equation for the wake potential where the driving term is the ultra-short bunch density, taking suitably into account the interplay between the sharpness and high energy of the bunch. Then, we show that a channel is formed longitudinally, through the externally injected beam while experiencing the effects of the bunch-driven plasma wake field, within the context of thermal wave model. The formation of the channel seems to be a final stage of the 3D evolution of the beam. This involves the appearance of small filaments and bubbles around the longitudinal axis. The bubbles coalesce forming a relatively stable axially-symmetric hollow beam structure.

1. Introduction

In this paper, we are going to investigate the physical conditions to generate the hollow structure by means of a plasma wake field (PWF) excitation mechanism similar to the laser wake field (LWF) excitation. We use a relativistic high energy ultra-short electron bunch as a driver, whose time duration ranges from sub-picoseconds to femtoseconds, and a moderately long charged particle beam as a driven system, whose time duration ranges from (10^3 – 10^2) femtoseconds. The hollow structure results from the interaction of the PWF generated by the ultra-short bunch with the driven beam. Here, we study numerically the evolution of the driven beam within the framework of the Thermal Wave Model (TWM) for charged particle beam propagation [1–6], where a Schrödinger-like equation governs the longitudinal spatio-temporal evolution of a complex wave function, whose squared modulus is proportional to the beam density. The adopted model equations constitute a pair of coupled partial differential equations comprising a Poisson-like equation and the Schrödinger-like equation, constructed in the following way.

We first consider a cylindrically symmetric relativistic ultra-short bunch moving along the z-axis at the velocity $\beta c\hat{z}\,(\beta \simeq 1)$. We denote with $\rho_b(z, r, t)$ the number density of the bunch where r is the cylindrical radial coordinate and t is the time coordinate. In order to get an equation for the wake potential energy, we perform the coordinate transformation $\xi = z - \beta ct,\ r' = r,\ \tau = ct$. Under this transformation the linearized Lorentz–Maxwell fluid equations of the "bunch+system" can be reduced to the following Poisson-like equation:

$$\left(\frac{\partial^2}{\partial \xi^2} + 1\right)\left(\frac{1}{\gamma_0^2}\frac{\partial^2}{\partial \xi^2} + \nabla_\perp^2 - 1\right)U_w = -\left(\frac{1}{\gamma_0^2}\frac{\partial^2}{\partial \xi^2} - 1\right)\frac{\rho_b}{n_0\gamma_0} \tag{1}$$

where $U_w(r,\xi) = -q\,\Omega(r,\xi)/m_0\gamma_0c^2$ is the dimensionless wake potential energy, $\Omega = (\beta A_{1z} - \phi_1)$ is the dimensional wake potential, A_{1z} is the longitudinal component of the perturbation of vector potential $\mathbf{A}_1$, ϕ_1 is the perturbations of scaler potential ϕ, respectively. Also, γ_0 is the leading order term of the relativistic factor $\gamma = (1-\beta^2)^{-1/2}$ and $q = -e$ is the charge of the bunch. To obtain Eq. (1) we first observed that $\nabla_\perp = \partial/\partial r = \partial/\partial r'$ and further assumed that, on the fast time scale, $\partial/\partial\tau = 0$, which imposes the quasi-electrostatic approximation. Therefore, Eq. (1) relates $U_w(\xi, r)$ to $\rho_b(\xi, r)$ during the early times (note that we have, for simplicity, replaced r' by r). Note also that, we have made the longitudinal and radial variables dimensionless with respect to the plasma wave number $k_{pe} \equiv \omega_{pe}/c$, viz., $\xi \to k_{pe}\xi$ and $r \to k_{pe}r$, where $\omega_{pe} = (4\pi n_0 e^2/m_0)^{1/2}$ is the electron plasma frequency.

* Corresponding author at: Dipartimento di Fisica, Università di Napoli "Federico II", Italy.
E-mail address: tanjia.fatema@gmail.com (F. Tanjia).

http://dx.doi.org/10.1016/j.nima.2016.04.005
0168-9002/

The Poisson-like equation is a partial differential equation to describe the collective PWF excitation mechanism relating the wake potential and the bunch density. It has been used to describe the PWF theory for an unmagnetized plasma [7]. It has also been extended to describe the PWF excitation mechanism for a magnetized plasma [3].

Eq. (1) differs from the standard one of PWF theory [7] and contains second and fourth order derivatives with respect to ξ. To obtain this equation, we have taken into account carefully the longitudinal sharpness of the bunch compared to its high energy conditions i.e., value of γ_0. Note that, our assumption of ultrashort electron bunch leads to the condition that the bunch length is much less than the plasma wavelength, i.e., $k_{pe}\sigma_z \lll 1$, where σ_z is the bunch length. Therefore, we are looking forward to study a regime where the ultra sharpness of the bunch length ($\partial/\partial\xi$) compensates the smallness of $1/\gamma_0$ in such a way that the term $|1/\gamma_0(\partial/\partial\xi)|$ in Eq. (1) could not be neglected and be comparable to 1. This leads to the condition $1/\gamma_0 \approx k_{pe}\sigma_z \lll 1$. To study the behavior of the wake potential from Eq. (1), this condition must be satisfied for any set of parameters.

We assume that a second cylindrically symmetric beam (i.e., *witness* or *driven* charged-particle beam), is launched toward the plasma wake along z-axis to experience the effects of the PWF produced by the driving bunch (i.e., ultra-short bunch). Here, the longitudinal spatiotemporal evolution of the driven beam manifests on longer time scales. In quantum-like domain (TWM), it is provided by the following Schrödinger-like equation, in plasma [1–5,9] as well as in conventional accelerators [8,10,11], beyond the quasi-electrostatic assumption, viz.,

$$i\epsilon\frac{\partial\psi}{\partial\tau} = -\frac{\epsilon^2}{2}\frac{\partial^2\psi}{\partial\xi^2} + U_w\psi \tag{2}$$

where $\psi(r, \xi, \tau)$ is the complex wave function called *beam wave function* and ϵ is the thermal beam emittance. Note that, we have made all the variables dimensionless with respect to k_{pe}, viz., $\tau \to k_{pe}\tau$, $\xi \to k_{pe}\xi$, $r \to k_{pe}r$, $\epsilon \to \epsilon k_{pe}$, and $\psi = \psi/k_{pe}^{3/2}$. Note also that $\rho_b'(r, \xi, \tau) = N|\psi(r, \xi, \tau)|^2$, where N is the total number of driven beam particles.

The pair of Poisson-like and Schrödinger-like equation, i.e., Eqs. (1) and (2), respectively, is analogous to the Zakharov-like coupled system of equations [12] (and references therein). It describes the spatiotemporal evolution of the driven beam while interacting with the plasma wake that has been generated by the ultra-short driving bunch. In the next section, we will present the numerical results of this coupled system of equations.

2. Numerical results

As we have already pointed out, Eq. (1) that governs the spatiotemporal evolution of the wake potential has been numerically integrated by assuming the Gaussian distribution in cylindrical symmetry, viz., $\rho_b(r, \xi) = n_b \exp\left[-\left(\frac{\xi^2}{2k_{pe}^2\sigma_z^2} + \frac{r^2}{k_{pe}^2\sigma_\perp^2}\right)\right]$, where σ_z and $\sigma_\perp$ are the bunch length and spot size of the driving bunch, respectively. The spatial distribution of the dimensionless wake potential energy $U_w(r, \xi)$ [normalized by $(n_b/n_0\gamma)$] is plotted as a function of dimensionless ξ and r.

Fig. 1 shows the longitudinal evolution of the normalized wake potential energy U_w and the corresponding longitudinal and radial gradients $\nabla_\xi U_w$ and $\nabla_r U_w$ respectively, in the vicinity of the longitudinal axis ($r \to 0$). The corresponding values of the bunch length and spot size (both normalized by k_{pe}) are considered as $\sigma_z \to k_{pe}\sigma_z \simeq 10^{-2}(\simeq 0.1\ \mu\text{m})$ and $\sigma_\perp \to k_{pe}\sigma_\perp \simeq 5.5(\simeq 50\ \mu\text{m})$, respectively. The normalization factor for U_w is $n_b/n_0\gamma \simeq 10^{-7}$ ($\gamma_0 \simeq 10^3$, $n_0 \simeq 10^{17}\ \text{cm}^{-3}$, and $n_b \simeq 10^{14}\ \text{cm}^{-3}$). All the parameters have been chosen in such a way to satisfy the condition $1/\gamma_0 \approx k_{pe}\sigma_z \lll 1$. The wake potential energy $U_w(\xi, 0)$ (blue line) and the corresponding longitudinal and radial gradients, i.e., $\nabla_\xi[U_w(\xi, 0)]$ (orange line) and $\nabla_r[U_w(\xi, 0)]$ (green line), respectively, exhibit regular oscillations along ξ. The longitudinal gradient is much greater than the radial one.

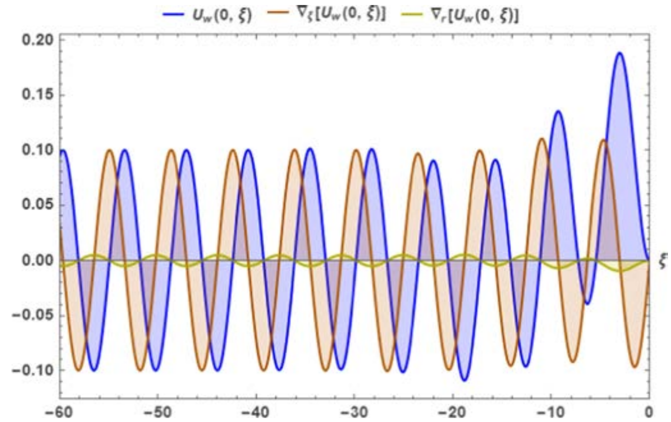

Fig. 1. Longitudinal evolution of the normalized wake potential energy U_w (blue curve) and the corresponding longitudinal and radial gradients $\nabla_\xi U_w$ (orange curve) and $\nabla_r U_w$ (green curve) respectively, in the vicinity of the longitudinal axis ($r \to 0$) for dimensionless bunch length $\sigma_z \to k_{pe}\sigma_z \simeq 10^{-2}(\simeq 0.1\ \mu\text{m})$ and spot size $\sigma_\perp \to k_{pe}\sigma_\perp \simeq 5.5(\simeq 50\ \mu\text{m})$. (For interpretation of the references to color in this figure caption, the reader is referred to the web version of this paper.)

Next, for the driven beam, we chose an initial normalized dimensionless Gaussian profile similar to the driving bunch but longitudinally off-set by the normalized length $\bar{\xi} \to k_{pe}\bar{\xi}$ at $\tau = 0$, of the form $\psi(r, \xi, 0) = \frac{1}{\sqrt{\sqrt{2\pi}\sigma_z'\pi\sigma_\perp'^2}} \exp\left[-\left(\frac{(\xi+\bar{\xi})^2}{4\sigma_z'^2} + \frac{r^2}{2\sigma_\perp'^2}\right)\right]$, where σ_z' and $\sigma_\perp'$ are the beam length and spot size, respectively, that are normalized by k_{pe}, viz., $\sigma_z' \to k_{pe}\sigma_z'$ and $\sigma_\perp' \to k_{pe}\sigma_\perp'$. For this initial beam profile, we numerically solve the Schrödinger-like Eq. (2), in which U_w is the output of numerical solution of Eq. (1). For the driven beam, we chose $\sigma_z' = 40$ and $\sigma_\perp' = 1000$ with an offset $\bar{\xi} = 80$ and $\epsilon = 10^{-3}$. Note that, we have chosen the normalized dimensionless beam length σ_z' in such a way that it is comparable to the wake field wavelength ($\sim 100\ \mu\text{m}$). In these conditions, we can assume that the self-interaction is negligible. Therefore, it is justified that in Eq. (2), we did not take into account the interaction of the driven beam on itself (self-interaction). In the next sections, we analyse the spatiotemporal evolution of the driven beam density $\rho_b'(r, \xi, \tau) = N|\psi(r, \xi, \tau)|^2$ in different dimensions, i.e., 1D, 2D, and 3D, respectively.

2.1. Density oscillations in 1D

Figs. 2 and 3 show the longitudinal oscillations of $\rho_b'(r, \xi, \tau)$ as a function of ξ at given r and τ, and radial oscillations as a function of r at given ξ and τ, respectively, for $\sigma_z' = 40$, $\sigma_\perp' = 1000$ with an initial Gaussian profile. The longitudinal oscillations are pronounced at the radial origin ($r \approx 0$) and start to decrease as r increases, as shown in Fig. 2. Note that, with increasing τ, starting from r=0 till 140 we observe decrements of the total particles through oscillations whilst between r=140 and r=280 we observe increment. The profiles at r=140 and r=280 for any τ overlap to reconstitute the initial condition. For a fixed r, the longitudinal density oscillations with respect to ξ are rapid in early τ and then reduce as τ increases. The radial oscillations of $\rho_b'(r, \xi, \tau)$ for fixed ξ and τ are clearly visible in Fig. 3. We have chosen the values of ξ in such a way that: the first ($\xi = -120$) is located in one σ_z' left from the Gaussian pick; the second ($\xi = -80$) is located at the Gaussian pick; finally, the third

Please cite this article as: F. Tanjia, et al., Nuclear Instruments & Methods in Physics Research A (2016), http://dx.doi.org/10.1016/j.nima.2016.04.005